Available online at www.sciencedirect.com
ScienceDirect
Advances in Space Research xxx (2007) xxx–xxx
ADVANCES IN SPACE RESEARCH (a COSPAR publication)
www.elsevier.com/locate/asr

# High resolution science with high redshift galaxies

R.A. Windhorst [a,*], N.P. Hathi [a], S.H. Cohen [a], R.A. Jansen [a], D. Kawata [b], S.P. Driver [c], B. Gibson [d]

[a] School of Earth & Space Exploration, Arizona State University, Box 871404, Tempe, AZ 85287-1404, USA
[b] Carnegie Observatories, 813 Santa Barbara Street, Pasadena, CA 91101, USA
[c] School of Physics and Astronomy, St. Andrews, Fife KY16 9SS, Scotland, United Kingdom
[d] University of Central Lancashire, Preston, Lancashire PR1 2HE, United Kingdom

Received 16 January 2007; received in revised form 2 July 2007; accepted 3 July 2007

**Abstract**

We summarize the high-resolution science that has been done on high redshift galaxies with Adaptive Optics (AO) on the world's largest ground-based facilities and with the Hubble Space Telescope (HST). These facilities complement each other. Ground-based AO provides better light gathering power and in principle better resolution than HST, giving it the edge in high spatial resolution imaging and high resolution spectroscopy. HST produces higher quality, more stable PSF's over larger field-of-views in a much darker sky-background than ground-based AO, and yields deeper wide-field images and low-resolution spectra than the ground. Faint galaxies have steadily decreasing sizes at fainter fluxes and higher redshifts, reflecting the hierarchical formation of galaxies over cosmic time. HST has imaged this process in great structural detail to $z \lesssim 6$, and ground-based AO and spectroscopy has provided measurements of their masses and other physical properties with cosmic time. Last, we review how the 6.5 m James Webb Space Telescope (JWST) will measure First Light, reionization, and galaxy assembly in the near–mid-IR after 2013.


*Keywords:* High resolution imaging; Distant galaxies; Galaxy assembly; Reionization; First Light; James Webb Space Telescope

## 1. Introduction

In this paper, we briefly review the current status of high resolution imaging of high redshift galaxies. In the last decade, major progress has been made with the Hubble Space Telescope (HST), and through targeted programs using Adaptive Optics (AO) on the world's best ground-based facilities. It is not possible to review all these efforts here, and so we refer the reader to more detailed reviews in proceedings by, e.g., Livio et al. (1998), Cristiani et al. (2000), Mather et al. (2006), Ellerbroek and Bonaccini Calia (2006), and Gardner et al. (2006).

## 2. What can and has been done from the ground?

High resolution AO-imaging on distant galaxies has been carried out successfully with large ground-based telescopes. A number of AO studies observed distant galaxies in the near-IR (e.g., Larkin et al., 2000, 2006; Glassman et al., 2002; Steinbring et al., 2004; Melbourne et al., 2005; Huertas-Company et al., 2007). Large ground-based telescopes with well calibrated AO *can* in principle match or supersede HST's resolution on somewhat brighter objects than accessible to HST, if AO guide stars are available in or nearby the AO field-of-view (FOV), as shown by Steinbring et al. (2004) (Fig. 1a and b here). Ground-based telescopes can also provide a much larger collecting area, allowing one to obtain higher spectral resolution, spatially-resolved spectra of faint galaxies (e.g., Larkin et al., 2006). This enables the study of the morphology and rotation curves of faint galaxies in order to measure their

* Corresponding author.
*E-mail address:* Rogier.Windhorst@asu.edu (R.A. Windhorst).

0273-1177/$30 © 2007 COSPAR. Published by Elsevier Ltd. All rights reserved.
doi:10.1016/j.asr.2007.07.005

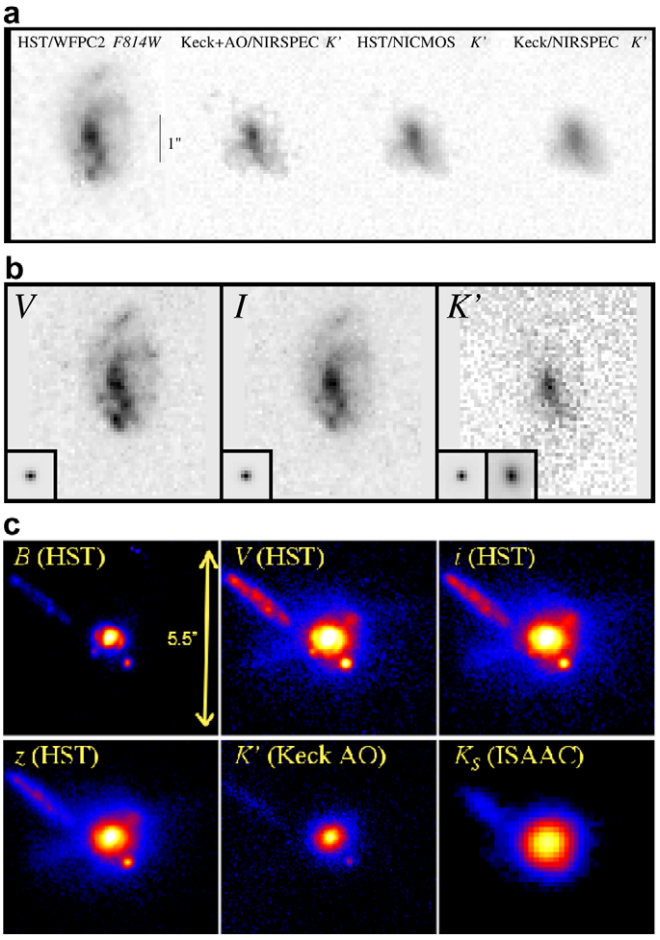


Fig. 1. (a and b) Comparison of Keck AO images of a spiral galaxy at $z = 0.531$ to HST V and I-band images, a simulated HST/NICMOS K′ image, and a Keck NIRSPEC image in natural seeing (from Steinbring et al., 2004). (c) Comparison of Keck AO images of a recent merger at $z = 0.61$ to HST and VLT/ISAAC images (from Melbourne et al., 2005).

masses and constrain galaxy assembly. Melbourne et al. (2005) used Keck AO and HST images to distinguish stellar populations, AGN and dust (Fig. 1c here). At longer wavelengths ($\lambda \gtrsim$ 1–2 μm), ground-based AO has provided PSF's that are as good as, or sharper than the $\lambda/D$ that the 2.4 m HST provides.

The PSF-stability and dynamic range, FOV, low sky-brightness and depth that diffraction limited space based images provide are difficult to match by ground-based AO imaging. There are two primary factors for this. First, atmospheric phase fluctuations (seeing) affect the Strehl ratio and PSF-stability, and therefore the effective dynamic range and FOV of ground-based AO images, compared to the diffraction limited PSF and FOV that the (aberration corrected) HST provides. Second, the sky-brightness at $\lambda \simeq$ 1–2 μm is typically $\sim 10^3\times$ (or ~7 mag) fainter in space compared to the ground (Thompson et al., 2006). The bright atmospheric OH-forest thus limits the surface brightness (SB) sensitivity that can be achieved from the ground, even with larger telescopes. Without AO, the deepest ground-based near-IR imaging achieved to date in the best natural seeing (~0.46″ FWHM) was done with VLT/ISAAC in the HDF-S (Labbé et al., 2003), reaching $J = 25.8$, $H = 25.2$ and $K_s = 25.2$ AB-mag ($7.5\sigma$) in ~35 h per filter. HST/NICMOS can reach these sensitivities in less than one hour, or could reach $\gtrsim 2$ mag deeper in the same amount of time. These VLT images would have gone deeper, had they been done with AO, but then they may not have covered a $2.5' \times 2.5'$ FOV. In conclusion, diffraction limited space-based imaging provides much darker sky over a wider FOV, more stable PSF's, better dynamic range, and therefore superior sensitivity. Ground-based AO is *complementary* to what space-based imaging can do. In the future, multi-conjugate AO (MCAO) from the ground will aim to provide nearly diffraction limited imaging over wider FOV's than possible with AO alone. Hence, MCAO facilities on 8–30 m telescopes may become competitive with HST and JWST at 1–2 μm wavelength in terms of PSF-width *and* FOV. This is why JWST no longer has cost-driving specifications below 1.7 μm wavelength, although it will probably perform quite well to 1.0 and possibly 0.7 μm. Future MCAO may not be competitive with space-based imaging in terms of PSF-stability, dynamic range, sky-brightness, and therefore sensitivity. In the thermal infrared ($\lambda \gtrsim 2$ μm), space-based imaging will be superior in depth. But to achieve the highest possible resolution on somewhat brighter objects, ground-based MCAO will be superior to space-based imaging. *It is critical for the future development of both space-based and ground-based high resolution imaging to keep this complementarity in mind, so that both sets of instruments can be developed to maximize the overall scientific return.*

## 3. Why does high resolution imaging need to be done from space?

The HST/ACS GOODS survey (Ferguson et al., 2004) showed that the median sizes of faint galaxies decline steadily towards higher redshifts (Fig. 2), despite the $\Theta$–$z$ rela-

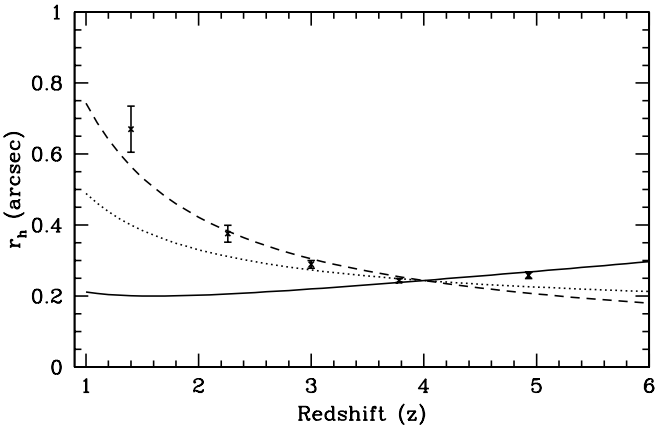


Fig. 2. Size evolution of galaxies in the HST GOODS fields (from Ferguson et al., 2004), indicated by the dashed and dotted curves, as summarized in Section 3. The solid curve indicates constant sizes in WMAP cosmology.

Please cite this article in press as: Windhorst, R.A. et al., High resolution science with high redshift galaxies, J. Adv. Space Res. (2007), doi:10.1016/j.asr.2007.07.005

tion that minimizes at $z \simeq 1.65$ in WMAP ΛCDM cosmology. While SB and other selection effects in these studies are significant, this figure suggests evidence for intrinsic size evolution of faint galaxies, where galaxy half-light radii $r_{hl}$ evolve approximately with redshift as: $r_{hl}(z) \propto r_{hl}(0) \cdot (1+z)^{-s}$ with $s \simeq 1$. This reflects the hierarchical formation of galaxies, where sub-galactic clumps and smaller galaxies merge over time to form the larger/massive galaxies that we see today (e.g., Navarro et al., 1996).

The HST/ACS Hubble UltraDeep Field (HUDF; Beckwith et al., 2006) showed that high redshift galaxies are intrinsically very small, with typical sizes of $r_{hl} \simeq 0.12''$ or 0.7–0.9 kpc at $z \simeq 4$–6. A combination of ground-based and HST surveys shows that the apparent galaxy sizes decline steadily from the RC3 to the HUDF limits (Fig. 3 here; Odewahn et al., 1996; Cohen et al., 2003; Windhorst et al., 2006). At the bright end, this is due to the survey SB-limits, which have a slope of +5 mag/dex in Fig. 3. At the faint end, ironically, this appears *not* to be exclusively due to SB-selection effects (cosmological

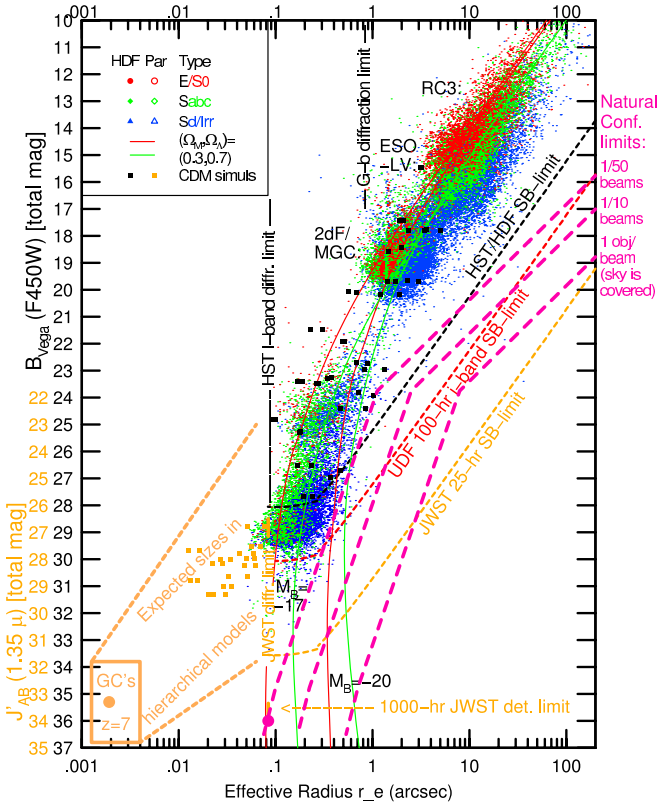


Fig. 3. Galaxy sizes vs. $B_{Vega}$ or $J_{AB}$-mag from the RC3 to the HUDF limit. Short dashed lines indicate survey limits for the HDF (black), HUDF (red), and JWST (orange): the point-source sensitivity is horizontal and the SB-sensitivity has slope = +5 mag/dex. Broken long-dashed pink lines indicate the natural confusion limit, below which objects begin to overlap due to their own sizes. Red and green lines indicate the expectations at faint fluxes of the *non-evolving* median size for RC3 elliptical and spiral galaxies, respectively (Odewahn et al., 1996). Orange and black squares indicate hierarchical size simulations (Kawata et al., 2004). Note that most galaxies at $J_{AB} \gtrsim 28$ mag are expected to be smaller than the HST and JWST diffraction limits (i.e. $r_{hl} \lesssim 0.1''$).

$(1+z)^4$ SB-dimming), since for $B_J \gtrsim 23$ mag the samples do *not* bunch up against the survey SB-limits. Instead it occurs because: (a) their hierarchical formation and size evolution (Fig. 2); (b) at $J_{AB} \gtrsim 26$ mag, one samples the faint end of the luminosity function (LF) at $z_{med} \gtrsim 2$–3, resulting in intrinsically smaller galaxies (Fig. 4b; Yan and Windhorst, 2004b); and (c) the increasing inability to properly deblend faint galaxies at fainter fluxes. This leads ultradeep surveys to slowly approach the "natural" confusion limit, where a fraction of the objects unavoidably overlaps with neighbors due to their finite *object size* (Fig. 3), rather than the finite instrumental resolution, which causes the *instrumental* confusion limit. Most galaxies at $J_{AB} \gtrsim 28$ mag are likely unresolved point-sources at $r_{hl} \lesssim 0.1''$ FWHM, as suggested by hierarchical size simulations in Fig. 3 (Kawata et al., 2004). This is why they are best imaged from space, which provides the best point-source and SB-sensitivity in the near-IR. The fact that many faint objects remain unresolved at the HST diffraction limit effectively reduces the $(1+z)^4$ SB-dimming to a $(1+z)^2$ flux-dimming (with potentially an intermediate case for partially resolved objects, or linear objects that are resolved in only one direction), mitigating the incompleteness of faint galaxy samples. The trick in deep HST surveys is therefore to show that this argument has not become circular, and that larger galaxies at high redshift are not missed. Other aspects that compound these issues are size-overestimation due to object confusion, size-bias due to the sky-background and due to image noise, which will be studied in detail elsewhere (e.g., Hathi et al., 2007).

## 4. What has been done with the hubble space telescope?

One of the remarkable discoveries by HST was that the numerous faint blue galaxies are in majority late-type (Abraham et al., 1996; Glazebrook et al., 1995; Driver et al., 1995) and small (Odewahn et al., 1996; Pascarelle et al., 1996) star-forming objects. They are the building blocks of the giant galaxies seen today. By measuring their distribution over rest-frame type versus redshift, HST has shown that galaxies of all Hubble types formed over a wide range of cosmic time, but with a notable transition around redshifts $z \simeq 0.5$–1.0 (Driver et al., 1998; Elmegreen et al., 2007). This was done through HST programs like the Medium-Deep Survey (Griffiths et al., 1994), GOODS (Giavalisco et al., 2004), GEMS (Rix et al., 2004), and COSMOS (Scoville et al., in press). Subgalactic units rapidly merged from the end of reionization to grow bigger units at lower redshifts (Pascarelle et al., 1996). Merger products start to settle as galaxies with giant bulges or large disks around redshifts $z \simeq 1$ (Lilly et al., 1998, in press). These evolved mostly passively since then, resulting in giant galaxies today, possibly because the epoch-dependent merger rate was tempered at $z \lesssim 1$ by the extra expansion induced by Λ (Cohen et al., 2003). To avoid caveats from the morphological K-correction (Giavalisco et al., 1996; Windhorst et al., 2002), galaxy structural classification needs to done

Please cite this article in press as: Windhorst, R.A. et al., High resolution science with high redshift galaxies, J. Adv. Space Res. (2007), doi:10.1016/j.asr.2007.07.005

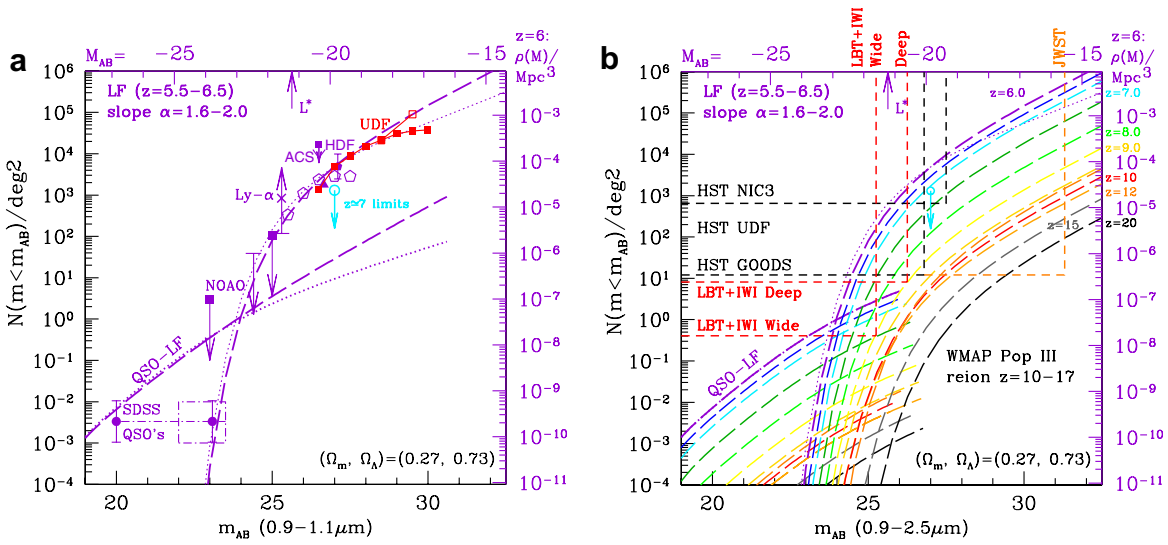


Fig. 4. (a) Integral luminosity function (LF) of $z \simeq 6$ objects, plotted as surface density vs. AB-mag. The $z \simeq 6$ LF may be very steep, with faint-end Schechter slope $|\alpha| \simeq 1.8$–$1.9$ (Yan and Windhorst, 2004b). Dwarf galaxies and not quasars therefore likely completed the reionization epoch at $z \simeq 6$ (Yan and Windhorst, 2004a). This is what JWST will observe in detail to AB ≃ 31.5 mag (1 nJy). (b) Possible extrapolation of the LF of Fig. 4a for $z$; $\gtrsim 7$, which is not yet constrained by data. Successive colors show redshift shells 0.5 in $\Delta z$ apart from $z = 6$, 6.5, …, 10, and also for $z = 12$, 15, 20. The HST/ACS has detected objects at $z \lesssim 6.5$, but its discovery space $A \cdot \Omega \cdot \Delta\log(\lambda)$ is limited to $z \lesssim 6.5$. NICMOS similarly is limited to $z \lesssim 8$ (Bouwens et al., 2004a,b; Yan and Windhorst, 2004a,b). JWST can trace the entire reionization epoch from First Light at $z \simeq 20$ to the end of reionization at $z \simeq 6$.

at rest-frame wavelengths longwards of the Balmer break at high redshifts (Taylor-Mager et al., 2007). JWST will make such studies possible with 0.1″–0.2″ FWHM resolution at observed near–IR wavelengths (1–5 μm), corresponding to the restframe-optical–near-IR at the median redshift of faint galaxies ($z_{\rm med} \simeq 1$–$2$; Mobasher et al., in press).

## 5. First Light, reionization & galaxy assembly with JWST

The James Webb Space Telescope (JWST) is designed as a deployable 6.5 m segmented IR telescope for imaging and spectroscopy from 0.6 μm to 28 μm. After its planned 2013 launch (Mather and Stockman, 2000), JWST will be automatically deployed and inserted into an L2 halo orbit. It has a nested array of sun-shields to keep its temperature at $\lesssim$40 K, allowing faint imaging to AB $\lesssim$ 31.5 mag ($\simeq$1 nJy) and low resolution (R$\simeq$100–1000) spectroscopy to AB $\lesssim$ 29 mag in the near – mid-IR. Further details on JWST are given by M. Clampin (this Volume).

### 5.1. First Light

The WMAP polarization results imply that the Dark Ages which started at recombination ($z \simeq 1089$) lasted until the First Light objects started shining at $z \lesssim 20$, and that the universe was first reionized at redshifts as early as $z \simeq 11$–$17$ (Spergel et al., 2003, 2007). The epoch of First Light is thought to have started with Population III stars of 200–300$M_\odot$ at $z \gtrsim 10$–$20$ (Bromm, 2003). Groupings of Pop III stars and possibly their extremely luminous supernovae should be visible to JWST at z ≃ 10–20 (Gardner et al., 2006).

This is why JWST needs NIRCam at 0.6–5 μm and MIRI at 5–28 μm. The First Light epoch and its embedded Pop III reionizing sources may have been followed by a delayed epoch of Pop II star-formation, since Pop III supernovae may have heated the IGM enough that it could not cool and form the IMF of the first Pop II stars until $z \lesssim 8$–$10$ (Cen, 2003). The IMF of Pop II stars may have formed in dwarf galaxies with masses of $10^6$–$10^9 M_\odot$ with a gradual onset between $z \simeq 9$ and $z \simeq 6$. The reionization history may have been more complex and/or heterogeneous, with some Pop II stars forming in sites of sufficient density immediately following their Pop III predecessors at $z \gtrsim 10$.

HST/ACS can detect objects at $z \lesssim 6.5$, but its discovery space $A \cdot \Omega \cdot \Delta\log(\lambda)$ cannot trace the entire reionization epoch. HST/NICMOS similarly is limited to $z \lesssim 8$ and provides limited statistics. HST/WFC3 can explore the redshift range $z \simeq 7$–$8$ with a wider FOV than NICMOS. Fig. 4b shows that with proper survey strategy (area *and* depth), JWST can trace the LF throughout the entire reionization epoch, starting with the first star-forming objects in the First Light epoch at $z \lesssim 20$, to the first star-forming dwarf galaxies at the end of the reionization epoch at $z \simeq 6$. Since in WMAP cosmology the amount of available volume per unit redshift decreases for $z \gtrsim 2$, the observed surface density of objects at $z \simeq 10$–$20$ will be small, depending on the hierarchical model used. This is illustrated in Fig. 4b, where the predicted surface densities at $z \simeq 7$–$20$ are uncertain by at least 0.5 dex. To observe the LF of First Light star-clusters and subsequent dwarf-galaxy formation may require JWST to survey GOODS-sized areas to AB ≃ 31.5 mag ($\simeq$1 nJy at 10-$\sigma$), using 7 filters for reliable photometric redshifts, since

Please cite this article in press as: Windhorst, R.A. et al., High resolution science with high redshift galaxies, J. Adv. Space Res. (2007), doi:10.1016/j.asr.2007.07.005

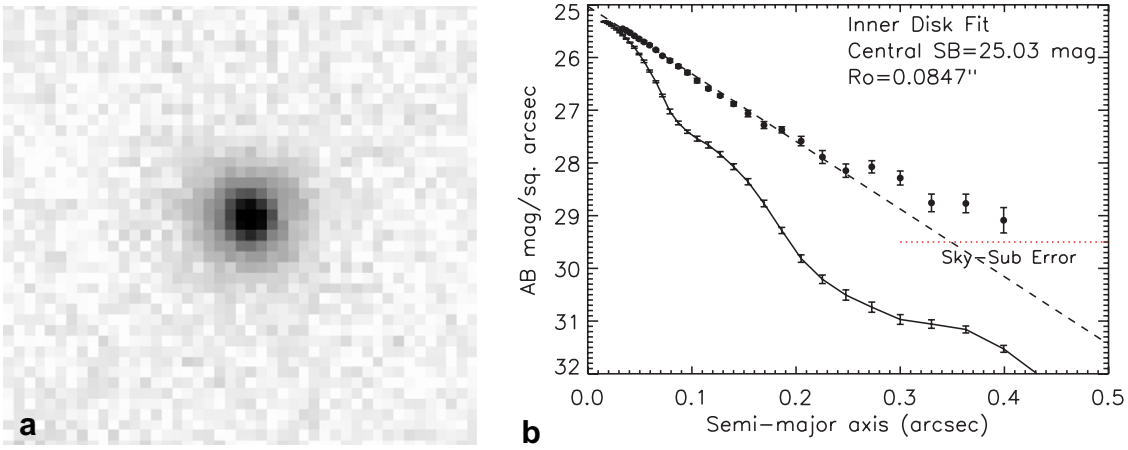


Fig. 5. (a) Sum of 49 *compact* isolated i-band dropouts in the HUDF, selected by Hathi et al. (2007) from the list of Yan and Windhorst (2004b). This image is equivalent to a 5000 hr HST $z$-band exposure – or a 330 h JWST 1 μm exposure – of an average compact isolated $z \simeq 6$ object. (b) The radial surface brightness profile of the image stack of Fig. 5a compared to the ACS PSF. The physical radius where the profile starts to deviate from a pure exponential profile (dashed) constrains the dynamical age to $\tau_{dyn} \simeq 100$–200 Myr at $z \simeq 6$, i.e., similar to the SED age.

objects with AB $\gtrsim$ 29 mag will be too faint for spectroscopy. Hence, JWST needs to have the quoted sensitivity/aperture (''*A*''; to reach AB $\gtrsim$ 31 mag), field-of-view (FOV = Ω; to cover GOODS-sized areas), and wavelength range (0.7–28 μm; to cover SED's from the Lyman to Balmer breaks at $z \gtrsim$ 6–20), as summarized in Fig. 4b.

### 5.2. Reionization

The HUDF data showed that the LF of $z \simeq 6$ objects is potentially very steep (Bouwens et al., 2006; Yan and Windhorst, 2004b), with a faint-end Schechter slope $|\alpha| \simeq 1.8$–1.9 after correcting for sample incompleteness (Fig. 4a). Deep HST/ACS grism spectra confirmed that 85–93% of HUDF i-band dropouts to $z_{AB} \lesssim 27$ mag are at $z \simeq 6$ (Malhotra et al., 2005). The steep faint-end slope of the $z \simeq 6$ LF implies that dwarf galaxies may have collectively provided enough UV-photons to complete reionization at $z \simeq 6$ (Yan and Windhorst, 2004a). This assumes that the Lyman continuum escape fraction at $z \simeq 6$ is as large as observed for Lyman-break Galaxies at $z \simeq 3$ (Steidel et al., 1999), which is reasonable – although not proven – given the expected lower dust content in dwarf galaxies at $z \simeq 6$. Hence, dwarf galaxies, and not quasars, likely completed the reionization epoch at $z \simeq 6$. The Pop II stars in dwarf galaxies therefore cannot have started shining *pervasively* much before $z \simeq$ 7–8, or no neutral H-I would be seen in the foreground of $z \gtrsim 6$ quasars (Fan et al., 2003), and so dwarf galaxies may have ramped up their formation fairly quickly from $z \simeq 9$ to $z \simeq 6$. A first glimpse of this may already be visible in the HUDF NICMOS surveys, which suggests a significantly *lower* surface density of $z \gtrsim 7$ candidates compared to $z \simeq 6$ objects (Bouwens et al., 2004a,b; Yan and Windhorst, 2004b; light blue upper limit in Fig. 4a and b), although the $\gtrsim$600 HST orbits spent on the HUDF only resulted in a few believable $z \gtrsim 7$ candidates at best. JWST surveys are designed to provide $\gtrsim 10^4$ objects at $z \simeq 7$ and 100's of objects in the epoch of First Light and at the start of reionization (Fig. 4b).

### 5.3. Galaxy assembly

JWST can measure how galaxies of all types formed over a wide range of cosmic time, by accurately measuring their distribution over rest-frame optical type and structure as a function of redshift or cosmic epoch. HST/ACS has made significant progress at $z \simeq 6$, surveying very large areas (GOODS, GEMS, COSMOS), or using very long integrations (HUDF, Beckwith et al., 2006). Fourier Decomposition (FD) is a robust way to measure galaxy morphology and structure in a quantitative way (Odewahn et al., 2002), where even Fourier components indicate symmetric parts (arms, bars, rings), and odd Fourier components indicate asymmetric parts (tidal features, spurs, lopsidedness, etc.). FD of nearby galaxies imaged with HST in the rest-frame UV (Windhorst et al., 2002) can be used to quantitatively measure the presence and evolution of bars, rings, spiral arms, and other structural features at higher redshifts (e.g., Jogee et al., 2004), and can be correlated to other classification parameters, such as CAS (Conselice, 2003). Such techniques will allow JWST to measure the detailed history of galaxy assembly in the epoch $z \simeq$ 1–3, when most of today's giant galaxies were made. JWST will be able to do this out to $z \simeq$ 10–15 at least (see Fig. 6 of Windhorst et al., 2006), hence enabling to quantitatively trace galaxy assembly. The rest-frame UV-morphology of galaxies is dominated by young and hot stars, as modulated by copious amounts of intermixed dust. This complicates the study of very high redshift galaxies. At longer wavelengths (2–28 μm), JWST will be able to map the effects from dust in star-forming objects at high redshifts.

Fig. 5a shows the sum of 49 *compact* isolated i-band dropouts in the HUDF (Yan and Windhorst, 2004b),

Please cite this article in press as: Windhorst, R.A. et al., High resolution science with high redshift galaxies, J. Adv. Space Res. (2007), doi:10.1016/j.asr.2007.07.005

which is a stack of about half the $z \simeq 6$ objects that have no obvious interactions or neighbors. These objects all have similar fluxes and half-light radii ($r_e$), so this image represents a 5000 h HST/ACS z-band exposure-stack on an "average compact isolated $z \simeq 6$ object", which is equivalent to a ~330 h JWST 1 μm exposure on *one* such object. Fig. 5b suggests that the radial SB-profile of this stacked image deviates from a pure exponential profile for $r \gtrsim 0.25''$, at SB-levels that are well above those corresponding to PSF and sky-subtraction errors. In hierarchical models, this physical scale-length may constrain the dynamical age of these compact isolated i-band $z \simeq 6$ dropouts, suggesting that $\tau_{dyn} \simeq$100–200 Myr for the typical galaxy masses seen at $z_{AB} \lesssim 29$ mag. This age is similar to stellar population age, as discussed in Hathi et al. (2007). This then suggests that the bulk of their stars observed at $z \simeq 6$ may have started forming at $z \lesssim$ 7–8. This is consistent with the double reionization model of Cen (2003), where the first reionization by Pop III stars at $z \simeq$ 10–20 is followed by a delayed onset of Pop II star-formation in dwarf galaxies at $z \lesssim 9$.

The red boundaries in Fig. 4b indicate part of the galaxy and QSO LF that a ground-based 8 m class telescope with a wide-field IR-camera can explore to $z \lesssim 9$ and AB $\lesssim$ 25 mag. A ground-based wide-field near-IR survey to AB $\lesssim$ 25–26 mag can sample $L \gg L^*$ galaxies at $z \lesssim 9$, which is an essential ingredient to study the co-evolution of supermassive black-holes and proto-bulges for $z \lesssim 9$, and an essential complement to the JWST First Light studies. The next generation of wide-field near-IR cameras on ground-based 8–10 m class telescopes can do such surveys over many $deg^2$ to AB $\simeq$ 25–26 mag, complementing JWST, which will survey GOODS-sized areas to AB $\lesssim$ 31.5 mag (red dashed lines in Fig. 4b).

## 6. Conclusions

High resolution imaging of high redshift galaxies is best done from space, because faint galaxies are small ($r_{hl} \lesssim 0.15''$), while the ground-based sky is too bright and the PSF not stable enough to obtain good high resolution images at faint fluxes (AB $\gtrsim$ 27 mag). Ground-based AO imaging can provide higher spatial resolution on brighter objects than space-based imaging. HST has led the study of galaxy assembly, showing that galaxies form hierarchically over time through repeated mergers with sizes growing steadily over time as $r_{hl}(z) \propto r_{hl}(0) \cdot (1+z)^{-s}$ and $s \simeq 1$. The Hubble sequence gradually emerges at $z \lesssim$ 1–2, when the epoch-dependent merger rate starts to wind down. The global onset of Pop II-star dominated dwarf galaxies ended the process of reionization at $z \simeq 6$. JWST will extend these studies into the epoch of reionization and First Light, and trace galaxy SED's in the rest-frame-optical for $z \lesssim 20$. In conclusion, high resolution imaging of high redshift galaxies has made significant steps forward with HST and recent ground-based AO facilities, and will see tremendous breakthroughs with JWST and MCAO in the future.

## Acknowledgements

This work was supported by HST Grants from STScI, which is operated by AURA for NASA under contract NAS 5-26555, and by NASA JWST Grant NAG 5-12460. Other JWST studies are at: www.asu.edu/clas/hst/www/jwst/. We thank Harry Ferguson, Jason Melbourne, and Eric Steinbring for helpful suggestions.

## References

Abraham, R.G., Tanvir, N.R., Santiago, B.X., et al. Galaxy morphology to $I = 25$ mag in the hubble deep field. MNRAS 279, L47–L52, 1996.
Beckwith, S.V.W., Stiavelli, M., Koekemoer, A.M., et al. The hubble ultra deep field. AJ 132, 1729–1755, 2006.
Ellerbroek, B.L. Bonaccini Calia, D., Advances in adaptive optics II. SPIE 6272, 2006.
Bouwens, R.J., Illingworth, G.D., Thompson, R.I., et al. Star formation at $z \sim 6$: the hubble ultra deep parallel fields. ApJ 606, L25–L28, 2004a.
Bouwens, R.J., Illingworth, G.D., Thompson, R.I., et al. Galaxies at $z \sim 7$–8: $z_{850}$-dropouts in the hubble ultra deep field. ApJ 616, L79–L82, 2004b.
Bouwens, R.J., Illingworth, G.D., Blakeslee, J.P., Franx, M. Galaxies at $z \sim 6$: the UV luminosity function and luminosity density from 506 HUDF, HUDF Parallel ACS Field, and GOODS *i*-dropouts. ApJ 653, 53–85, 2006.
Bromm, V. The formation of the first luminous objects in the universe. Ap&SS 284, 349–352, 2003.
Cen, R. The Universe was reionized twice. ApJ 591, 12–37, 2003.
Cohen, S.H., Windhorst, R.A., Odewahn, S.C., et al. The Hubble Space Telescope WFPC2 B-band parallel survey: a study of galaxy morphology for magnitudes $18 \leqslant B \leqslant 27$. AJ 125, 1762–1783, 2003.
Conselice, C.J. The relationship between stellar light distributions of galaxies and their formation histories. ApJS 147, 1–28, 2003.
Cristiani, S., Renzini, A., Williams, R.E., Deep fields, in: Proceedings of the ESO Workshop held at Garching, Germany, 9–12 October 2000. ESO Astroph. Symp. Springer-Verlag, Berlin, ISBN 3-540-42799-6, 2001.
Driver, S.P., Windhorst, R.A., Ostrander, E.J., et al. The morphological mix of field galaxies to $M_I = 24.25$ mag ($b_J \sim 26$ mag) from a deep Hubble Space Telescope WFPC2 image. ApJ 449, L23–L27, plus 2 plates, 1995.
Driver, S.P., Fernández-Soto, A., Couch, W.J., et al. Morphological number counts and redshift distributions to $I < 26$ from the hubble deep field: implications for the evolution of ellipticals, spirals, and irregulars. ApJ 496, L93–L96, plus 2 color plates, 1998.
Elmegreen, D.M., Elmegreen, B.G., Ravindranath, S., Coe, D.A. Resolved galaxies in the hubble ultra deep field: star formation in disks at high redshift. ApJ 658, 763–777, 2007.
Fan, X., Strauss, M.A., Schneider, D.P., et al. A survey of $z > 5.7$ quasars in the Sloan digital sky survey. II. Discovery of three additional quasars at $z > 6$. AJ 125, 1649–1659, 2003.
Ferguson, H.C., Dickinson, M., Giavalisco, M., et al. The size evolution of high-redshift galaxies. ApJ 600, L107–L110, 2004.
Gardner, J.P., Mather, J.C., Clampin, M., et al. The James Webb Space Telescope. Space Sci. Rev. 123, 485–606, 2006.
Giavalisco, M., Livio, M., Bohlin, R.C., et al. On the morphology of the HST faint galaxies. AJ 112, 369–377, plus 7 plates, 1996.
Giavalisco, M., Ferguson, H.C., Koekemoer, A.M., et al. The great observatories origins deep survey: initial results from optical and near-infrared imaging. ApJ 600, L92–L98, 2004.

Glassman, T.M., Larkin, J.E., Lafrenière, D. Morphological evolution of distant galaxies from adaptive optics imaging. ApJ 581, 865–875, 2002.

Glazebrook, K., Ellis, R., Sanriago, B., Griffith, R. The morphological identification of the rapidly evolving population of faint galaxies. MNRAS 275, L19–L22, 1995.

Griffiths, R.E., Casertano, S., Ratnatunga, K.U., et al. The morphology of faint galaxies in medium deep survey images using WFPC2. ApJ 435, L19–L22, 1994.

Hathi, N.P., Jansen, R.A., Windhorst, R.A., et al. Surface brightness profiles of composite images of compact galaxies at $z \simeq 4$–6 in the HUDF. AJ, in press, 2007.

Huertas-Company, M., Rouan, D., Soucail, G., et al. Morphological evolution of $z \sim 1$ galaxies from deep K-band AO imaging in the COSMOS deep field. A&A 468, 937, 2007.

Jogee, S., Barazza, F.D., Rix, H.-W., et al. Bar evolution over the last 8 billion years: a constant fraction of strong bars in the GEMS Survey. ApJ 615, L105–L108, 2004.

Kawata, D., Gibson, B.K., Windhorst, R.A. Cosmological simulations of the high-redshift radio universe. MNRAS 354, 387–392, 2004.

Labbé, I., Franx, M., Rudnick, G., et al. Ultradeep near-infrared ISAAC observations of the hubble deep field south: observations, reduction, multicolor catalog, and photometric redshifts. AJ 125, 1107–1123, 2003.

Larkin, J.E., Glassman, T.M., Wizinowich, P., et al. Exploring the structure of distant galaxies with Adaptive Optics on the Keck II telescope. PASP 112, 1526–1531, 2000.

Larkin, J., Barczys, M., Krabbe, A., et al. OSIRIS: a diffraction limited integral field spectrograph for Keck. New Astron. Rev. 50, 362–364, 2006.

Lilly, S., Schade, D., Ellis, R., et al. Hubble Space Telescope imaging of the CFRS and LDSS redshift surveys. II. Structural parameters and the evolution of disk galaxies to $z \sim 1$. ApJ 500, 75–94, 1998.

Lilly, S.J., Le Fèvre, O., Renzini, A., et al., zCOSMOS: a large VLT/VIMOS redshift survey covering $0 < z < 3$ in the COSMOS field. ApJS. Available from: <astro-ph/0612291>, in press.

Livio, M., Fall, S.M., Madau, P., The Hubble Deep Field, in: Proceedings of the STScI Symposium held in Baltimore MD, 6–9 May 1997. STScI Symp. Series No. 11, Cambridge University Press, New York, ISBN 0-521-63097-5, 1998.

Malhotra, S., Rhoads, J.E., Pirzkal, N., et al. An overdensity of galaxies at $z = 5.9 \pm 0.2$ in the hubble ultra deep field confirmed using the ACS grism. ApJ 626, 666–679, 2005.

Mather, J.C., Stockman, H.S. Next Generation Space Telescope, in: Breckinridge, J.B., Jakobsen, P. (Eds.), UV, Optical, and IR Space Telescopes and Instruments, vol. 4013. SPIE, pp. 2–16, 2000.

Mather, J.C., MacEwen, H.A. de Graauw, M.W.M., Space telescopes and instrumentation. I. Optical, infrared, and millimeter. SPIE vol. 6265, 2006.

Melbourne, J., Wright, S.A., Barczys, M., et al. Merging galaxies in GOODS-S: first extragalactic results from Keck Laser Adaptive Optics. ApJ 625, L27–L30, 2005.

Mobasher, B., Capak, P., Scoville, N.Z., et al., Photometric redshifts of galaxies in COSMOS. ApJS Available from: <astro-ph/0612344>, in press.

Navarro, J.F., Frenk, C.S., White, S.D.M. The structure of cold dark matter halos. ApJ 462, 563–575, 1996.

Odewahn, S.C., Windhorst, R.A., Driver, S.P., Keel, W.C. Automated morphological classification in deep Hubble Space Telescope UBVI fields: rapidly and passively evolving faint galaxy populations. ApJ 472, L13–L16, 1996.

Odewahn, S.C., Cohen, S.H., Windhorst, R.A., Philip, N.S. Automated galaxy morphology: a Fourier approach. ApJ 568, 539–557, 2002.

Pascarelle, S.M., Windhorst, R.A., Keel, W.C., Odewahn, S.C. Sub-galactic clumps at a redshift of 2.39 and implications for galaxy formation. Nature 383, 45–50, 1996.

Rix, H.-W., Barden, M., Beckwith, S.V.W., et al. GEMS: galaxy evolution from morphologies and SEDs. ApJS 152, 163–173, 2004.

Scoville, N.Z., Aussel, H., Brusa, M, et al., The Cosmic Evolution Survey (COSMOS) – overview. ApJS. Available from: <astro-ph/0612305>, in press.

Spergel, D.N., Verde, L., Peiris, H.V., et al. First-year Wilkinson Microwave Anisotropy Probe (WMAP) observations: determination of cosmological parameters. ApJS 148, 175–194, 2003.

Spergel, D.N., Bean, R., Doré, O., et al. Three-year Wilkinson Microwave Anisotropy Probe (WMAP) observations: implications for cosmology. ApJS 170, 377–408, 2007.

Steidel, C.C., Adelberger, K.L., Giavalisco, M., et al. Lyman-break galaxies at $z \gtrsim 4$ and the evolution of the ultraviolet luminosity density at high redshift. ApJ 519, 1–17, 1999.

Steinbring, E., Metevier, A.J., Norton, S.A., et al. Keck Adaptive Optics imaging of $0.5 < z < 1$ field galaxies from the Hubble Space Telescope Archive. ApJS 155, 15–25, 2004.

Taylor-Mager, V.A., Conselice, C.J., Windhorst, R.A., Jansen, R.A. Dependence of galaxy structure on rest-frame wavelength and galaxy type. ApJ 659, 162–187, 2007.

Thompson, R.I., Eisenstein, D., Fan, X., et al. Star formation history of the hubble ultra deep field: comparison with the Hubble Deep Field-North. ApJ 647, 787–798, 2006.

Windhorst, R.A., Taylor, V.A., Jansen, R.A., et al. A Hubble Space Telescope survey of the mid-ultraviolet morphology of nearby galaxies. ApJS 143, 113–158, 2002.

Windhorst, R.A., Cohen, S.H., Jansen, R.A., et al. How JWST can measure first light, reionization and galaxy assembly. New Astron. Rev. 50, 113–120, 2006.

Yan, H., Windhorst, R.A. The major sources of the cosmic reionizing background at $z \simeq 6$. ApJ 600, L1–L5, 2004a.

Yan, H., Windhorst, R.A. Candidates of $z \simeq 5.5$–7 galaxies in the Hubble Space Telescope Ultra Deep Field. ApJ 612, L93–L96, 2004b.

Please cite this article in press as: Windhorst, R.A. et al., High resolution science with high redshift galaxies, J. Adv. Space Res. (2007), doi:10.1016/j.asr.2007.07.005